

**An accurate and transferable machine learning interatomic
potential for equimolar and non-equimolar high-entropy
diborides**

Hong Meng, Yiwen Liu, Hulei Yu^{*}, Lei Zhuang, Yanhui Chu^{*}

School of Materials Science and Engineering, South China University of

Technology, Guangzhou, 510641, China

^{*}Corresponding author.

E-mail address: huleiyu@scut.edu.cn (H. Yu)

E-mail address: chuyh@scut.edu.cn (Y. Chu)

Abstract

Machine learning interatomic potentials have become a powerful tool to achieve molecular dynamics (MD) simulations with the accuracy of *ab initio* methods while beyond their length and timescale limitations. Here, we develop an efficient moment tensor potential (MTP) for high-entropy diborides (HEBs) based on unary and binary diborides with Ti-V-Cr-Zr-Nb-Mo-Hf-Ta-W principal elements. Notably, the trained MTP exhibits exceptional generalization across both equimolar and non-equimolar HEBs, with testing errors in energy and force of 2.6 meV/atom and 155 meV/Å for equimolar HEBs, and 3.7 meV/atom and 172 meV/Å for non-equimolar HEBs, respectively, indicating its remarkable accuracy and transferability. The reliability of the established MTP is further confirmed by a comparative analysis with first-principles calculations, where our MTP accurately reproduces the structural and mechanical properties of various HEBs. The work presents a significant advancement in the simulation of high-entropy ceramics with enhanced efficiency and accuracy.

Keywords: High-entropy borides, moment tensor potential, first-principles calculations, molecular dynamics.

1. Introduction

High-entropy borides, a class of inorganic compound solid solutions with one or more Wyckoff sites shared by no less than four principal elements, have attracted growing research interest due to their potential applications in both structural and functional fields.¹⁻³ Since the first report of 2016, a diverse range of high-entropy borides, including high-entropy monoborides,^{4,5} high-entropy diborides (HEBs),⁶⁻¹³ and high-entropy hexaborides,¹⁴⁻¹⁷ have been developed to show superior performance in thermal, mechanical, electromagnetic, and electrochemical characteristics, especially in extreme environments.¹⁻⁴ Among these materials, HEBs are considered highly anticipated candidates for applications in aerospace, cutting tools, and nuclear reactors owing to the combination of physical-chemical properties inherent to their constituent diborides, such as ultrahigh melting point, notable hardness, and outstanding chemical inertness.⁶⁻¹² However, the huge composition space of HEBs poses a significant challenge in exploring new materials with remarkable properties. Thus, theory-assisted simulations, including the first-principles calculations and molecular dynamics (MD) simulations, are deemed as effective solutions to the material discovery in HEBs.¹⁸⁻²⁰ Nevertheless, the computational cost and scalability issues of the first-principles methods greatly limit their further applications with complex systems,^{21,22} and the absence of reasonable interatomic potentials for HEBs in MD also poses a major obstacle to their wider implementation.

With the development of machine learning algorithms and data science, machine learning interatomic potentials (MLIPs) based on first-principles calculations have

become increasingly popular.^{10,23} These MLIPs simultaneously own the accuracy in the first-principles calculation level and efficiency in the MD simulation level. Up to now, several efforts have been successfully made in investigating the diborides via different MLIPs. Daw et al.²⁴ were pioneers in proposing a Tersoff-type MLIP for ZrB₂ and HfB₂ to investigate a variety of properties. Lin et al.²⁵ took a step further by fitted a moment tensor potential (MTP) for TiB₂ to simulate the mechanical response of monocrystals until failure. On the basis of the embedded atom method (EAM), Zalizniak et al.²⁶ enabled the construction of MLIPs for various metal diborides MB₂ (M = Al, Mg, Mo, Hf, Nb, Sc, Ti, Y, Zr, V). However, the development of MLIPs for HEBs remains in the early stages. To the best of our knowledge, the only instance of the MLIP construction for a specific quinary equimolar HEB was reported by Dai et al.¹⁰, utilizing a large-scale training dataset comprising 47000 configurations of this HEB. Consequently, it is highly urgent to develop an accurate and broadly applicable MLIP for various HEBs.

In this work, a highly transferable MTP for HEBs has been constructed based on density functional theory (DFT) calculations. Following our previously reported strategy,²⁷ the training dataset was effectively generated from unary and binary diborides with nine principal elements of group IVB, VB, and VIB. The accuracy and transferability of the trained MTP were well-examined by both the equimolar and non-equimolar HEB testing datasets to demonstrate low root mean square errors (RMSEs) in both energies and forces. Furthermore, the comparison of lattice parameters and mechanical properties between MD simulations with the fitted MLIP and DFT calculations was conducted to explore the reliability of our trained MTP. The successful

development of the highly transferable MTP offers a promising avenue to achieve efficient simulations in more complex HEBs.

2. Computational details

The first-principles calculations were implemented in the Vienna *Ab Initio* Simulation Package (VASP) based on the DFT with the projector augmented wave method (PAW)²⁸ and the Perdew-Burke-Ernzerhof (PBE)²⁹ version of the generalized gradient approximation (GGA).³⁰ The cutoff energy for the plane-wave basis of all calculations was set to 450 eV, and the convergence criteria for ionic and electronic steps were set to 10^{-3} and 10^{-4} eV, respectively. In addition, a spacing of 0.3 \AA^{-1} with the Γ -centered mesh was used in Brillouin zones, and the spin polarization effects were taken into account.³¹ Based on the TiB_2 conventional cell with a space group of $P6/mmm$, $3 \times 3 \times 4$, $2 \times 2 \times 4$, $2 \times 2 \times 5$, $2 \times 2 \times 6$, $2 \times 2 \times 7$, and $4 \times 4 \times 2$ supercells were built for unary (as well as binary and nonary), quaternary, quinary, senary, septenary, and octonary diborides, respectively. The special quasi-random structure (SQS) approach,³² implemented in the Alloy Theoretic Automated Toolkit (ATAT),³³ was utilized to mimic the chemical disorder in models for binary diborides and HEBs. Nine transition metal (TM) principal elements were selected from group IVB, VB, and VIB, i.e., Ti, V, Cr, Zr, Nb, Mo, Hf, Ta, and W. All the structures were fully relaxed before the calculations of the elastic tensor by the energy-strain approach.

The *ab initio* molecular dynamics (AIMD) calculations were further carried out with merely Γ point considered in Brillouin zones to generate different configurations. A timestep of 3 fs for up to 2000 steps was utilized in the NPT ensemble at 1000, 2000,

and 3000 K, respectively.

The MTP was constructed using the Machine Learning Interatomic Potentials (MLIP-3) packages with structural information on energies, forces, and stresses.²³ The training datasets were built according to the simple and efficient strategy for high-entropy ceramics reported in our previous work²⁷, which only required collection from DFT static calculations of unary and equimolar binary diborides with nine TM elements from AIMD. As there are nine compositions in unary diborides and 36 compositions in equimolar binary diborides, a total of 45 kinds of diborides were considered in the training dataset. For each composition at each temperature, 25 configurations were collected for training (a total of 3375 configurations) and five configurations for validation (a total of 675 configurations). Meanwhile, 50 equimolar and 50 non-equimolar HEBs with varied principal elements were randomly generated, with two configurations collected from each to build equimolar and non-equimolar testing datasets (300 configurations for each dataset). To ensure the accuracy and efficiency of the MTP, the cutoff radius (R_{cut}) and the maximum level (lev_{max})³⁴ were set to 6.5 Å and 22, respectively.

The MD simulations were performed in the Large-scale Atomic/Molecular Massively Parallel Simulator (LAMMPS) package,³⁵ interfaced with our trained MTP. All simulation models included 3000 atoms, with cationic sites randomly occupied by nine TM elements with corresponding ratios. The timestep in all MD simulations was set to 1 fs, and the damping parameters for temperature and pressure were set to 0.1 ps and 1 ps, respectively. Lattice constants were fully optimized with 20000 steps in the

NPT ensemble under 0 Pa and 300 K, and the temperature-dependent elastic tensors were computed by the evaluation of the Born matrix under 300 K.³⁶

3. Results and discussion

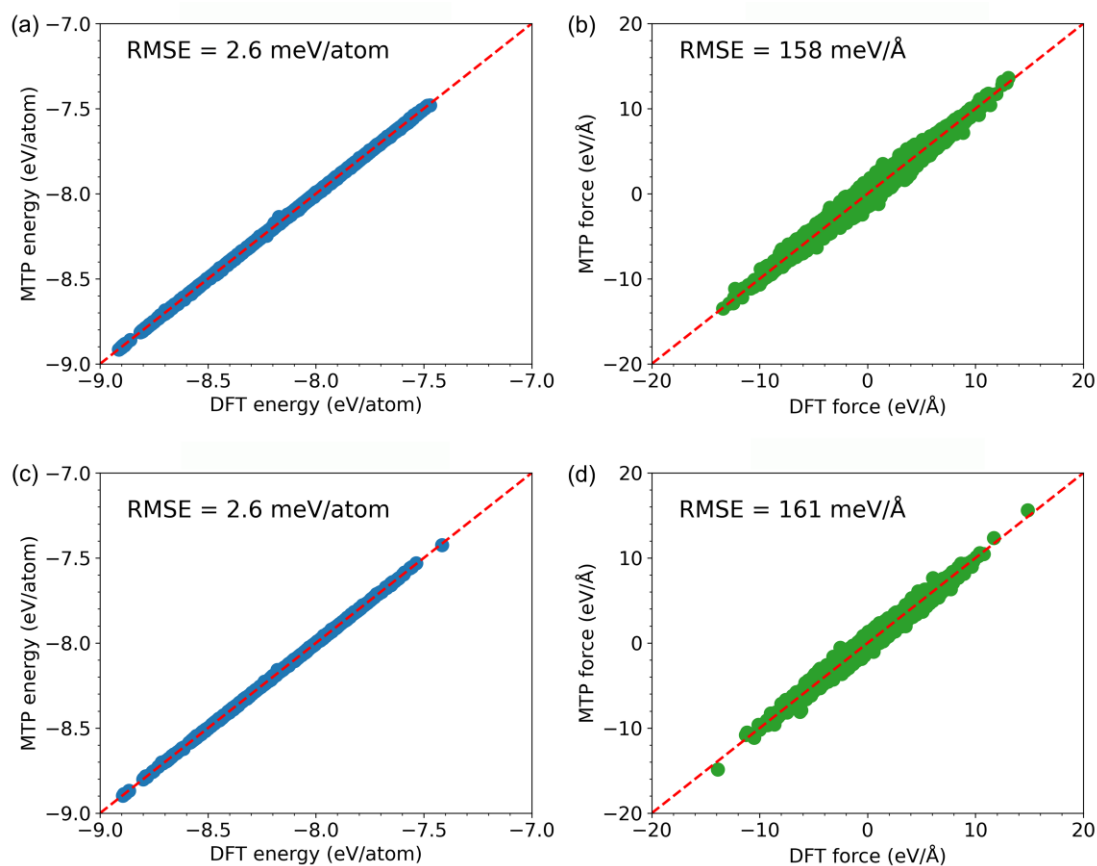


Fig. 1 Comparison of predicted energy and force between MTP and DFT calculations. RMSE of (a) energy and (b) force for the training dataset. RMSE of (c) energy and (d) force for the unary and binary diboride testing dataset.

The performance of the obtained MTP on training is first evaluated. As depicted in **Fig. 1**, there are almost no changes in RMSEs for the energy and force predictions for both the training (Fig.1(a-b)) and testing datasets (Fig.1(c-d)) of the unary and binary diborides, which are consistently low, being approximately 2.6 meV/atom for

energy and 158-161 meV/Å for force, respectively, suggesting the well-established MTP.

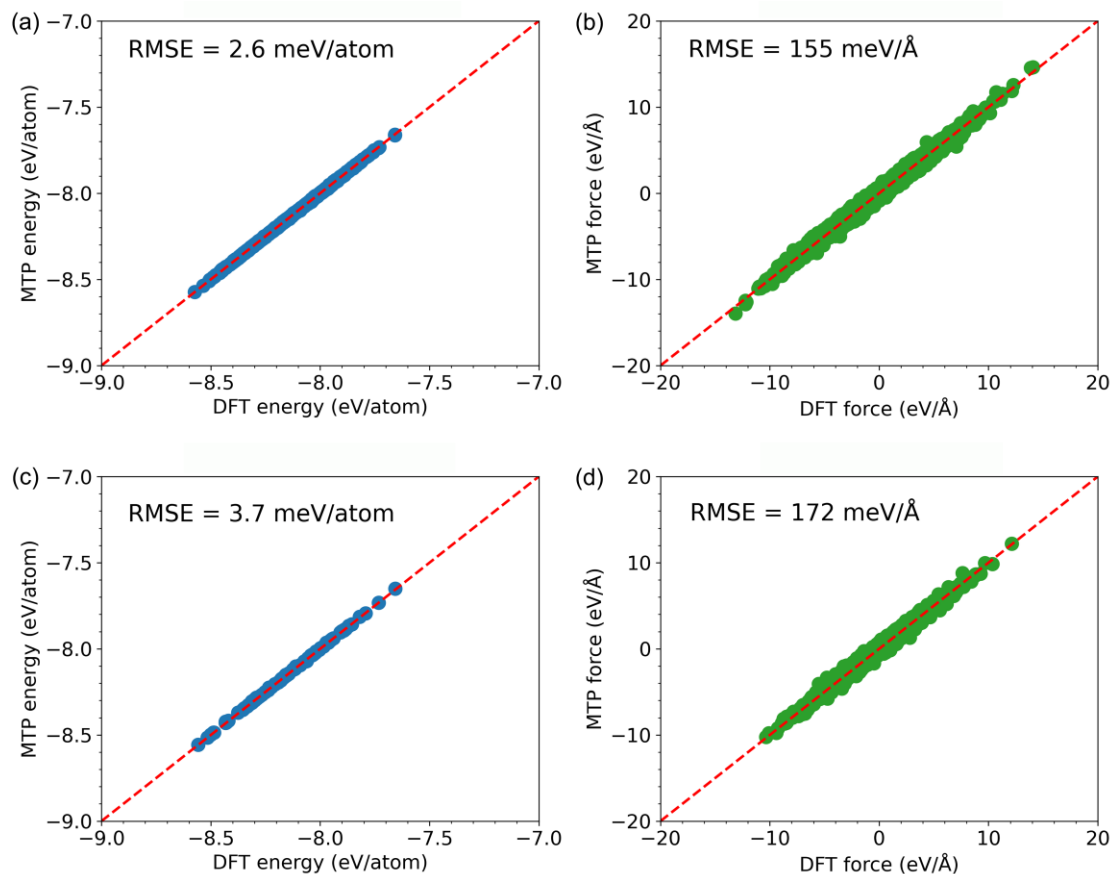


Fig. 2 Comparison of predicted energy and force between MTP and DFT calculations. RMSE of (a) energy and (b) force for the equimolar HEB testing dataset. RMSE of (c) energy and (d) force for the non-equimolar HEB testing dataset.

The applicability of the fitted MTP to equimolar and non-equimolar HEBs is also explored. As shown in **Fig. 2**, there are no significant discrepancies in the testing accuracies between the equimolar and non-equimolar HEB testing datasets, and both datasets have low RMSEs, achieving 2.6 meV/atom and 155 meV/Å for equimolar HEBs (see Fig.2 (a-b)) and 3.7 meV/atom and 172 meV/Å for energy and force for non-

equimolar HEBs (see Fig.2 (c-d)), respectively. It should be noted that these RMSEs are comparable to those of the training datasets, indicating the high accuracy and generalization performance of the fitted MTP. In addition, the accuracy of our fitted MTP is significantly higher than those of the previously reported MLIPs,^{10,37,38} further confirming the high accuracy of our fitted MTP. Based on these observations, it can be concluded that our trained MTP for HEBs is well-established, exhibiting high efficiency, accuracy, and transferability.

To further investigate the applicability of the trained MTP, the predictions on various properties in HEBs were carried out. **Fig. 3** presents a comparative analysis between MD simulations and DFT calculations, focusing on lattice parameters (a and c), elastic tensor (c_{11} , c_{12} , c_{13} , c_{33} , and c_{44}), bulk modulus (B), and shear modulus (G). It is found that the lattice constants obtained through MD simulations with our trained MTP are in good agreement with those derived from DFT calculations, indicating a high accuracy of our trained MTP. In addition, there still exist some small discrepancies in the predictions between the two methods, e.g., a slight underestimation is observed in two specific elastic parameters (C_{11} and C_{13}), as well as B with MD simulations compared to those from DFT calculations. These discrepancies may be attributed to the temperature difference (300 K in MD and 0 K in DFT) and different evaluation methodologies in the calculations of elastic tensors. Therefore, our trained MTP is significantly reliable for MD simulations. Despite these minor deviations, the overall consistency between MD and DFT results confirms the reliability of our trained MTP for MD simulations.

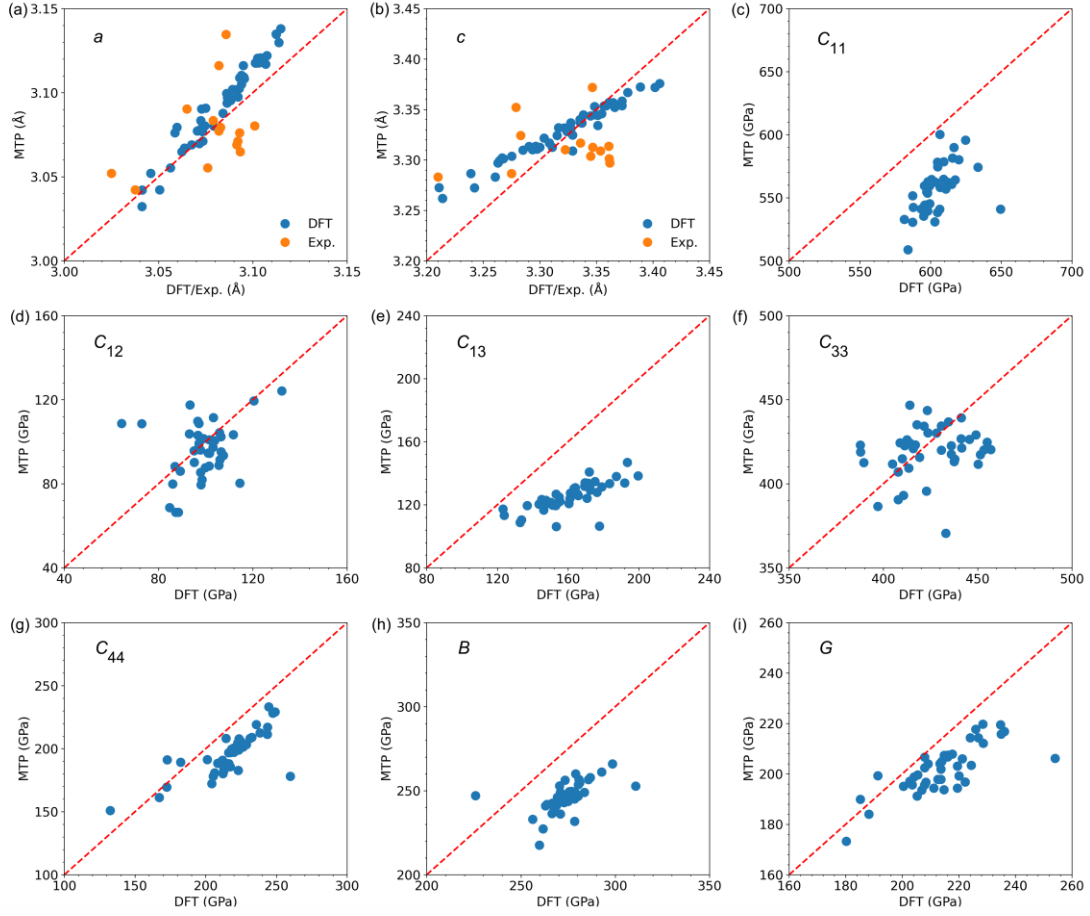


Fig. 3 Comparison of (a, b) lattice parameters, (c-g) elastic parameters, and (h, i) bulk and shear modules between MD simulations and DFT calculations.

4. Conclusion

In summary, an efficient, accurate, and transferable MTP applicable to HEBs with up to nine TM principal elements has been developed based on 3375 configurations from unary and equimolar binary diborides. The RMSEs for energy and force predictions across datasets (unary and binary diborides for training, equimolar and non-equimolar HEB for testing) exhibit consistently low values of 2.6, 2.6, and 3.7 meV/atom, respectively, for energy, and 158, 155, and 172 meV/Å, respectively, for force. These results demonstrate the remarkable accuracy and transferability of the

trained MTP in unary and binary diborides, as well as HEBs with varied compositions. The comparison of the structural and mechanical properties between MD simulations and DFT calculations further revealed the reliability of our trained MTP. Our work presents an efficient, accurate, and transferable MTP, enabling the realization of property screening on various HEBs.

Acknowledgements

We acknowledge the financial support from the National Key Research and Development Program of China (No. 2021YFA0715801), the National Natural Science Foundation of China (No. 52122204), and Guangzhou Basic and Applied Basic Research Foundation (SL2023A04J00690).

Author Contributions

Y. Chu conceived and designed this work. H. Meng, Y. Liu, and H. Yu performed the theoretical calculations. Y. Chu, H. Yu, and H. Meng analyzed the data and wrote the manuscript. All authors commented on the manuscript.

Competing Interests

The authors declare no competing financial interest.

Data Availability

The data that support the findings of this study are available from the corresponding author upon reasonable request.

References

1. Gild J, Zhang Y, Harrington T, Jiang S, Hu T, Quinn MC, et al. High-entropy metal diborides: a new class of high-entropy materials and a new type of ultrahigh temperature ceramics. *Sci Rep.* 2016;6:37946.
2. Oses C, Toher C, Curtarolo S. High-entropy ceramics. *Nat Rev Mater.* 2020;5(4):295-309.
3. Ma M, Ye B, Han Y, Sun L, He J, Chu Y. High-pressure sintering of ultrafine-grained high-entropy diboride ceramics. *J Am Ceram Soc.* 2020;103(12):6655-58.
4. Qin M, Yan Q, Wang H, Hu C, Vecchio K, Luo J. High-entropy monoborides: towards superhard materials. *Scripta Mater.* 2020;189:101-05.
5. Zhao P, Zhu J, Li M, Shao G, Lu H, Wang H, et al. Theoretical and experimental investigations on the phase stability and fabrication of high-entropy monoborides. *J Eur Ceram Soc.* 2023;43(6):2320-30.
6. Liu D, Wen T, Ye B, Chu Y. Synthesis of superfine high-entropy metal diboride powders. *Scripta Mater.* 2019;167:110-14.
7. Tallarita G, Licheri R, Garroni S, Orrù R, Cao G. Novel processing route for the fabrication of bulk high-entropy metal diborides. *Scripta Mater.* 2019;158:100-04.
8. Kirnbauer A, Wagner A, Moraes V, Primetzhofer D, Hans M, Schneider JM, et al. Thermal stability and mechanical properties of sputtered (Hf,Ta,V,W,Zr)-diborides. *Acta Mater.* 2020;200:559-69.
9. Feng L, Monteverde F, Fahrenholtz WG, Hilmas GE. Superhard high-entropy AlB_2 -type diboride ceramics. *Scr Mater.* 2021;199:113855.

10. Dai F, Sun Y, Wen B, Xiang H, Zhou Y. Temperature dependent thermal and elastic properties of high entropy $(\text{Ti}_{0.2}\text{Zr}_{0.2}\text{Hf}_{0.2}\text{Nb}_{0.2}\text{Ta}_{0.2})\text{B}_2$: molecular dynamics simulation by deep learning potential. *J Mater Sci Technol.* 2021;72:8-15.
11. Tang Z, Wen Z, Liu Y, Zhuang L, Yu H, Chu Y. Rapid experimental screening of high-entropy diborides for superior oxidation resistance. *Adv Funct Mater.* 2023;34:2312239.
12. Wen Z, Tang Z, Liu Y, Zhuang L, Yu H, Chu Y. Ultrastrong and high thermal insulating porous high-entropy ceramics up to 2000 °C. *Adv Mater.* 2024;36:2311870.
13. Meng H, Yu R, Tang Z, Wen Z, Yu H, Chu Y. Formation ability descriptors for high-entropy diborides established through high-throughput experiments and machine learning. *Acta Mater.* 2023;256:119132.
14. Chen H, Zhao Z, Xiang H, Dai F, Zhang J, Wang S, et al. Effect of reaction routes on the porosity and permeability of porous high entropy $(\text{Y}_{0.2}\text{Yb}_{0.2}\text{Sm}_{0.2}\text{Nd}_{0.2}\text{Eu}_{0.2})\text{B}_6$ for transpiration cooling. *J Mater Sci Technol.* 2020;38:80-85.
15. Qin M, Yan Q, Liu Y, Wang H, Wang C, Lei T, et al. Bulk high-entropy hexaborides. *J Eur Ceram Soc.* 2021;41(12):5775-81.
16. Ma M, Yang X, Meng H, Zhao Z, He J, Chu Y. Nanocrystalline high-entropy hexaboride ceramics enable remarkable performance as thermionic emission cathodes. *Fundam Res.* 2023;3:979-987.
17. Meng H, Tang Z, Bai H, Fu Y, Yu H, Chu Y. Accelerating the discovery of high-

entropy hexaborides by data-driven prediction: From equimolar to non-equimolar.

J Am Ceram Soc. 2024. <https://doi.org/10.1111/jace.19922>

18. Ye B, Wen T, Nguyen M, Hao L, Wang C, Chu Y, First-principles study, fabrication and characterization of $(\text{Zr}_{0.25}\text{Nb}_{0.25}\text{Ti}_{0.25}\text{V}_{0.25})\text{C}$ high-entropy ceramics. *Acta Mater.* 2019;170:15-23.
19. Liu Y, Yu H, Meng H, Chu Y, Atomic-level insights into the initial oxidation mechanism of high-entropy diborides by first-principles calculations. *J Materiomics.* 2024;10(2):423-430.
20. Zhao S, Lattice distortion in high-entropy carbide ceramics from first-principles calculations. *J Am Ceram Soc.* 2021;104(4):1874-1886.
21. Mellor W, Kaufmann K, Dippo O, Figueroa S, Schrader G, Vecchio K, Development of ultrahigh-entropy ceramics with tailored oxidation behavior. *J Eur Ceram Soc.* 2012;41(12):5791-5800.
22. Qin M, Vega H, Zhang D, Adapa S, Wright A, Chen R, Luo J, 21-Component compositionally complex ceramics: Discovery of ultrahigh-entropy weberite and fergusonite phases and a pyrochlore-weberite transition. *J Adv Ceram.* 2022;11(4):641-655.
23. Podryabinkin E, Garifullin k, Shapeev A, Novikov I. MLIP-3: Active learning on atomic environments with moment tensor potentials. *J Chem Phys.* 2023;159:084112.
24. Daw M, Lawson J, Bauschlicher C. Interatomic potentials for zirconium diboride and hafnium diboride. *Comput Mater Sci.* 2011;50:2828-2835.

25. Lin S, Casillas-Trujillo L, Tasnadi F, Hultman L, Mayrhofer P, Sangiovanni D, et al. Machine-learning potentials for nanoscale simulations of tensile deformation and fracture in ceramics. *npj Comput Mater.* 2024;10:67.
26. Zalizniak V, Zolotov O, Sidorov K. Interatomic potential for metal diborides. *Mol Simul.* 2021;47: 982-987.
27. Liu Y, Meng H, Zhu Z, Yu H, Zhuang L, Chu Y, An efficient strategy to construct general machine learning potentials for high-entropy ceramics, arXiv preprint arXiv, 2024.
28. Blöchl PE. Projector augmented-wave method. *Phys Rev B.* 1994;50:17953.
29. Kresse G, Furthmüller J. Efficiency of ab-initio total energy calculations for metals and semiconductors using a plane-wave basis set. *Comput Mater Sci.* 1996;6:15.
30. Perdew JP, Burke K, Ernzerhof M. Generalized gradient approximation made simple. *Phys Rev Lett.* 1996;77:3865.
31. Monkhorst HJ, Pack JD. Special points for Brillouin-zone integrations. *Phys Rev B.* 1976;13:5188.
32. Zunger A, Wei SH, Ferreira LG, Bernard JE. Special quasirandom structures. *Phys Rev Lett.* 1990;65:353.
33. Walle A. Multicomponent multisublattice alloys, nonconfigurational entropy and other additions to the alloy theoretic automated toolkit. *Calphad.* 2009;33:266-278.
34. Novikov I, Gubaev K, Podryabinkin E, Shapeev A. The MLIP package: Moment tensor potentials with MPI and active learning. *Mach Learn: Sci Technol.* 2021;2:025002.

35. Plimpton S. Fast parallel algorithms for short-range molecular dynamics. *J Comput Phys.* 1995;117:1-19.
36. Workum K, Gao G, Schall J. D, Harrison A. J. Expressions for the stress and elasticity tensors for angle-dependent potentials. *J Chem Phys.* 2006;125:144506.
37. Liu Y, Mo Y. Assessing the accuracy of machine learning interatomic potentials in predicting the elemental orderings: A case study of Li-Al alloys. *Acta Mater.* 2023;268:119742.
38. Dai F, Wen B, Sun Y, Xiang H, Zhou Y. Theoretical prediction on thermal and mechanical properties of high entropy $(Zr_{0.2}Hf_{0.2}Ti_{0.2}Nb_{0.2}Ta_{0.2})C$ by deep learning potential. *J Mater Sci Technol.* 2020;43:168-174.